ARCHIVES of FOUNDRY ENGINEERING

Published quarterly as the organ of the Foundry Commission of the Polish Academy of Sciences

ISSN (1897-3310)
Volume 8
Special Issue
3/2008

5 – 8

1/3

ATD and DSC analyses of nickel superalloys

F. Binczyk[a,*], J. Śleziona[a], J. Cwajna[b], S. Roskosz[b]
[1]Department of Metal Alloys and Composites Engineering,
[2]Department of Materials Science,
Silesian University of Technology, Krasińskiego Str. 8, 40-019 Katowice, Poland
* Corresponding author. E-mail address: franciszek.binczyk@polsl.pl

Received 23.06.2008; accepted in revised form 25.06.2008

Abstract

The study presents the results of investigations of phase transformations that take place during melting and solidification of nickel superalloys, like RENE 77, IN7 13C, MAR 247 and IN 100. Examinations were carried out by the ATD method of thermal analysis and DSC scanning calorimetry. It has been concluded that ATD offers wider possibilities for interpretation of the solidification process at its first stage, when from the liquid state the primary phases of a low heat of solidification are precipitating. The calorimetric method is more useful in the investigation of solid state phase transformations. The obtained values of the solidification parameters (T_{lik} and T_{sol}) are comparable for both methods, especially as regards alloys solidification. An undeniable advantage of the DSC method is the possibility to measure the value of the heat (enthalpy) of phase transformations, especially during melting of alloys.

Keywords: Nickel superalloys, ATD analysis, DSC analysis, Temperature, Solidification, Microstructure, Carbides

1. Introduction

Creep-resistant nickel alloys are the base material used for cast parts of aircraft engines, both static parts as well as the rotating guiding elements, operating at high temperatures under the effect of mass forces [1-3]. The requirements imposed on these castings include, among others, high fatigue resistance, creep resistance at high temperatures, and resistance to corrosion in media containing products of fuel combustion. The castings are made in near-net-shape moulds by investment process. Currently, the investment castings for parts of aircraft engines are being made from the modern family of nickel and cobalt alloys, including – among others – the following materials: IN-100, IN-713C, RENE77 and MAR-M257. These are the precipitation hardened alloys in which, during solidification, a specific type of macrostructure is produced. This is the macrostructure composed of equiaxial grains, frozen and columnar, with precipitates of primary carbides inside the grains and on the grain boundaries. In a structure of this type cracks may form and propagate, causing fatal failure in aircraft engines [4, 5]. Then the service life of an engine is considerably reduced and the performance costs increase.

World's technical literature provides abundant information on the methods of refining the macro- and microstructure of nickel superalloys by the technique of refining [6] and inoculation with nanoparticle inoculants [7-9].

Yet, to be able to control the microstructure formation and properties of the ready products, it is necessary to know first the phenomena that take place during solidification of these alloys. This mainly refers to the temperature of the beginning of solidification, the temperature range of the primary phases and matrix solidification, and the temperature of solid state transformations. This, in turn, enables choosing the best temperature of pouring when alloy has still sufficient castability and ability to faithfully reproduce the casting configuration. It is also necessary to ensure low shrinkage and low tendency to the formation of shrinkage cavities, which may happen when the temperature of mould pouring is too high.

2. Materials and methods of investigation

Investigations were carried out on nickel alloys which, besides nickel, contained the following main elements: **Rene 77:** 14,49% Co, 14,28% Cr, 4,42% Al, 4,20% Mo, 3,38% Ti, **IN-713C: 0,03% Co**, 13,26% Cr, 5,85% Al, 4,10% Mo, **0,85% Ti**, 2,27% **(Nb + Ta)**, **MAR-M247:** 10,01% Co, 8,47% Cr, 5,63% Al, 0,69% Mo, 1,02% Ti, **10,07% W**, **3,27% Ta, 1,40% Hf**, **IN-100:** 13,47% Co, 8,52% Cr, 5,76% Al, 2,98% Mo, 4,69% Ti, **0,82% V**.

The investigated alloys differ in the presence or absence and/or content of the alloying constituents marked in bold typing. Each alloy has additions of Cr, Al., Mo and Ti. Hence it can be concluded that the solidification process of these alloys will to a great extent depend on the presence and content of the above mentioned constituents, especially as regards the temperature T_{lik} and solidification range. Usually, before this stage is reached, there is a nucleation and crystallisation of primary phases, which in the majority of cases are intermetallic phases or primary carbides. The alloys contain carbon in amounts from 0,09 to 0,16%.

Melts were prepared in a VSG-02 induction furnace (made by Balzers) using an Al_20_3 crucible. The charge weight was about 1,2 kg. Melting was carried out under protective argon atmosphere kept at a pressure of about 10013 hPa. The temperature of molten metal was controlled by an immersion Pt-PtRh10 thermocouple. The pouring temperature ranged from 1560 to 1580°C.

The solidification process was recorded by a Crystaldigraph PC-8T apparatus. Schematic representation of the research stand is shown in Figure 1.

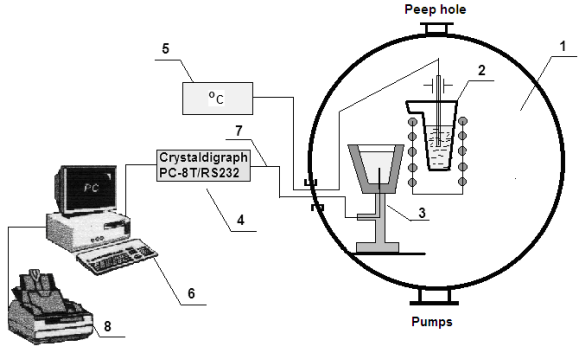

Fig. 1. Schematic representation of a research stand: 1- chamber of VSG-02 furnace; 2- crucible and induction coil; 3 – graphite foundry mould; 4 – Crystaldigraph PC-8T apparatus; 5 – digital temperature measuring unit; 6 – PC computer; 7 – compensation lead; 8 – printer

Calorimetric examinations were also carried out. For the determination of temperature range and thermal effects of phase transformations a differential scanning Multi HTC S60 calorimeter was used. The weight of samples was similar and varied from 310 to 340 mg. Tests were made under the protective argon atmosphere at the heating and cooling rate of 10°C/min. The samples were preheated to 1450°C

3. The results of investigations

An example of the thermal analysis curve plotted for IN-713C alloy is shown in Figure 2.

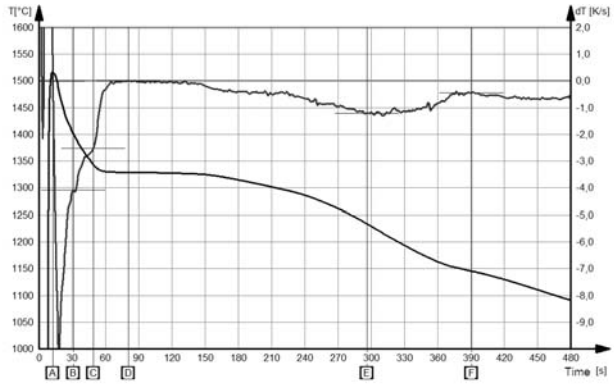

Characteristic points :

[A]	12,5 [s]	1515,7 [°C]	-0,01 [K/s]	0,00 [K/s2]*e-3
[B]	31,0 [s]	1400,8 [°C]	-4,08 [K/s]	0,00 [K/s2]*e-3
[C]	49,0 [s]	1343,8 [°C]	-2,52 [K/s]	0,00 [K/s2]*e-3
[D]	80,5 [s]	1329,0 [°C]	0,00 [K/s]	0,00 [K/s2]*e-3
[E]	296,0 [s]	1233,8 [°C]	-1,20 [K/s]	0,00 [K/s2]*e-3
[F]	390,5 [s]	1145,5 [°C]	-0,45 [K/s]	0,00 [K/s2]*e-3

Fig. 2. Plotted curve of ATD analysis and values measured at points characteristic of IN-713C alloy

From ATD curves, the basic parameters of alloy solidification were determined and compared in Table 1.

Table 1.
The results of ATD analysis

Alloy	T_{max} °C	T_c °C	T_{liq} °C	T_{sol} °C	T_{st} °C
RENE-77	1533	1402	1328	1221	1071
IN-713C	1516	1401	1329	1234	1145
MAR-247	1502	1430	1343	1282	1191
IN-100	1540	1398	1315	1280	-

Where the individual symbols stand for:
T_{max} – maximum temperature,
T_c – solidification temperature of carbide phases,
T_{liq} – temperature of the beginning of metallic matrix solidification,
T_{sol} – temperature of the end of alloy solidification,
T_s – temperature of solid state transformations.

Plotted results of DSC analysis for IN713C alloy sample heating and cooling are shown in Figs. 3 and 4.

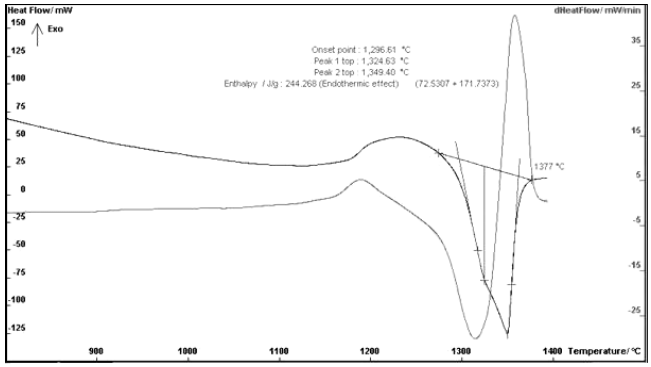

Fig. 3. The DSC diagram of IN 713C alloy heating

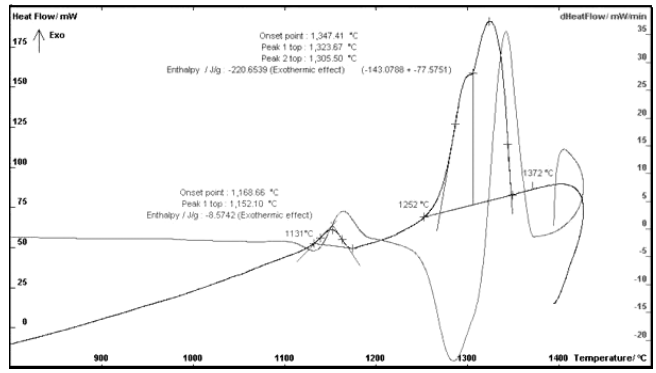

Fig. 4. The DSC diagram of IN 713C alloy cooling

The results obtained from the curves of calorimetric analysis are compared in Tables 2 and 3 for alloy heating and cooling, respectively.

Table 2.
Temperature and heat of transformation in heating DSC diagram

Alloy	Solid state				Liquid state				
	T_s ^0C	T_{max} ^0C	T_f ^0C	+Q J/g	T_{sol} ^0C		T_{liq} ^0C	T_c ^0C	+Q J/g
IN 100	1193	1214	1232	6,16	1290		1336	1365	230,16
IN 713C	no data available				phase B	1297	1349	1377	72,53
					phase A	1325			171,74
MAR 247	1191	1215	1236	2,34	1324		1368	1395	234,97
RENE 77	no data available				phase B	1274	1352	1386	31,59
					phase A	1302			237,41

Table 3.
Temperature and heat of transformation in cooling DSC diagram

Alloy	Liquid state					Solid state			
	T_c ^0C		T_{liq} ^0C	T_{sol} ^0C	-Q J/g	T_s ^0C	T_{max} ^0C	T_f ^0C	-Q J/g
IN 100	1350	phase A	1304		-54,77	1224	1193	1176	-2,92
		phase B	1287	1238	-166,44				
IN 713C	1372	phase A	1324		-143,01	1169	1152	1131	-8,57
		phase B	1305	1252	-77,58				
MAR 247	1386	phase A	1346		-37,20	1251	1244	1211	-0,91
		phase B	1327	1255	-174,25	1211	1188	1170	-4,93
RENE 77 A	1368	phase A	1319		-190,95	1155	1134	1075	-3,87
		phase B	1275	1245	-19,43				

Note: Ts - initial temperature, T_f - end temperature

4. Discussion of results

Examples of microstructures obtained for IN-713C and MAR 247 alloys in unetched state are shown in Figs. 5 and 6.

Microstructural examinations of the discussed nickel alloys confirm the exothermic heat effect observed on ATD curves and caused by the solidification of primary phases. Probably these are the primary carbides of an MC type. The above refers in particular to the RENE 77 and IN 100 alloys. In MAR 247 and IN 713C, apart from carbides of this type, one can also see carbides of the chain-like distribution and carbides in the form of "Chinese script".

It can be expected that the said carbides will be of secondary type, or they may have precipitated at the end of the solidification process as a eutectic phase.

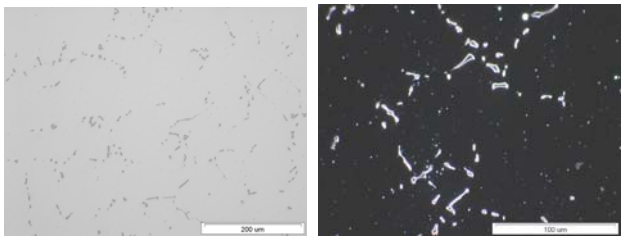

Fig. 5. Microstructure of IN-713C alloy. Typical "chain-like" distribution of carbides

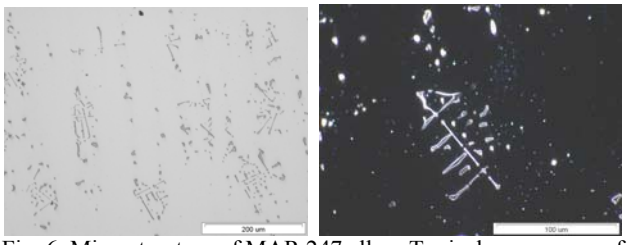

Fig. 6. Microstructure of MAR 247 alloy. Typical appearance of carbides as a "Chinese script"

Basing on the obtained results of investigations, the characteristic solidification parameters obtained by ATD and DSC were compared. The results are shown in Figs. 7 and 8.

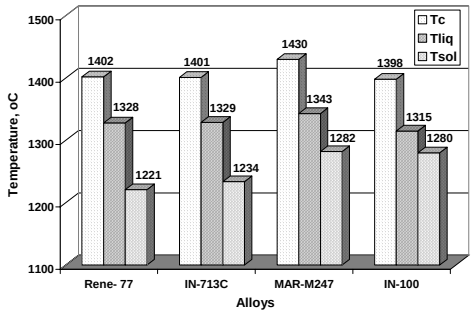

Fig. 7. A comparison of characteristic temperature values during solidification determined by the method of ATD analysis

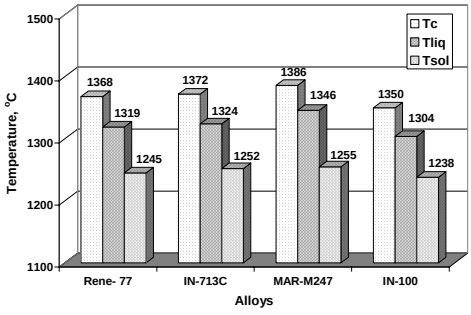

Fig. 8. A comparison of characteristic temperature values during solidification determined by the method of DSC analysis

This statement is well confirmed by the results of DSC analysis. The plotted curves show an exothermic effect in solid state, particularly well visible in MAR 247 alloy.

The obtained results enable drawing a conclusion that the ATD method of thermal analysis offers more possibilities for interpretation of the first stage of solidification process when in liquid metal the primary phases of a low heat of solidification are precipitating. In DSC method, because of a very small weight of the samples, these effects cannot be observed.

The calorimetric method, on the other hand, seems to be more useful in the investigation of solid state phase transformations. The values of the solidification parameters (T_{lik} and T_{sol}) obtained by both methods are comparable, especially during alloy solidification. An undeniable advantage of the DSC method is the possibility to measure the value of the heat (enthalpy) of phase transformations, especially during melting of alloys.

The studies were done under a Commissioned Research Project PBZ-MNiSW–03/I/2007 financed by the Ministry of Science and Higher Education.

References

[1] F. Zupanic, T. Boncina, A. Krizman, F.D. Tichelaar: Structure of continuously cast Ni-based superalloy Inconel 713C, Journal of Alloys and Compounds, v. 329, issue 1-2, (2001), pp.290-297.

[2] M. Tabuchi, K. Kubo, K. Yagi, A.T. Yokobori Jr, A. Fuji: Results of a Japanese round robin on creep crack growth evaluation methods for Ni-base superalloys, Engineering Fracture mechanics, volume 62, issue 1, (1999), pp. 47-60.

[3] Superalloys, Metal Powder Report, v. 51, issue 9, (1996), p.39.

[4] A. Smith, A. Mainwood, M. Watkins: The kinetics of the capture of nitrogen by nickel defects in diamond, Diamond and related materials, v. 11, issue 3-6, (2002), pp. 312-315.

[5] M. Lachowicz: Characteristics of microstructural changes and crack formation mechanism detected during welding and heat treatment of Inconel 713C superalloy, Doctor's Thesis, Politechnika Wrocławska (2006) (in Polish).

[6] Hartman D., Muerrle U., Reber G.: The effects of electron beam refining on the cast ability of IN 713 C, Metal, (1992), issue 5, pp. 443-447.

[7] L. Liu, T. Huang, Y. Xiong: Grain refinement of superalloy K4169 by addition of refiners: cast structure and refinement mechanisms, Materials Science and Engineering A, 394, (2005), pp.1-8.

[8] Y. Xiong, J. Du, X. Wie, A. Yang, L. Liu: Grain refinement of Superalloy IN 718C by the addition of Inoculants, Metallurgical and Materials Transactions A, vol. 35A, July (2004), pp. 2111-2114.

[9] Y. Xiong, A. Yang, Y. Guo, W. Liu, L. Liu: Grain refinement of superalloys K3 and K4169 by the addition of refiners, Science and Technology of Advanced Materials, issue 2, (2001), pp. 13-17.